

Targeting of amacrine cell neurites to appropriate synaptic laminae in the developing zebrafish retina

Leanne Godinho¹, Jeff S. Mumm¹, Philip R. Williams¹, Eric H. Schroeter¹, Amy Koerber¹, Seung W. Park², Steven D. Leach² and Rachel O. L. Wong^{1,*}

¹Department of Anatomy and Neurobiology, Washington University School of Medicine, 660 South Euclid Avenue, Box 8108, St Louis, MO 63110, USA

²Departments of Surgery, Oncology and Cell Biology, Johns Hopkins Medical Institutions, Baltimore, MD 21287, USA

*Author for correspondence (e-mail: wongr@pcg.wustl.edu)

Accepted 5 September 2005

Development 132, 5069-5079

Published by The Company of Biologists 2005

doi:10.1242/dev.02075

Summary

Cellular mechanisms underlying the precision by which neurons target their synaptic partners have largely been determined based on the study of projection neurons. By contrast, little is known about how interneurons establish their local connections *in vivo*. Here, we investigated how developing amacrine interneurons selectively innervate the appropriate region of the synaptic neuropil in the inner retina, the inner plexiform layer (IPL). Increases (ON) and decreases (OFF) in light intensity are processed by circuits that are structurally confined to separate ON and OFF synaptic sublaminae within the IPL. Using transgenic zebrafish in which the majority of amacrine cells express fluorescent protein, we determined that the earliest amacrine-derived neuritic plexus formed between two cell populations whose somata, at maturity, resided on opposite sides of this plexus. When we followed the behavior of

individual amacrine cells over time, we discovered that they exhibited distinct patterns of structural dynamics at different stages of development. During cellular migration, amacrine cells exhibited an exuberant outgrowth of neurites that was undirected. Upon reaching the forming IPL, neurites extending towards the ganglion cell layer were relatively more stable. Importantly, when an arbor first formed, it preferentially ramified in either the inner or outer IPL corresponding to the future ON and OFF sublaminae, and maintained this stratification pattern. The specificity by which ON and OFF amacrine interneurons innervate their respective sublaminae in the IPL contrasts with that observed for projection neurons in the retina and elsewhere in the central nervous system.

Key words: Amacrine, Stratification, Retina, Interneuron, IPL

Introduction

The establishment of precise synaptic connections is crucial to the proper functioning of the central nervous system (CNS). Insights into how synaptic specificity is achieved come largely from studies of projection neurons whose synaptic targets are located at great distances – for example, the projections of retinal ganglion cell axons to the tectum or colliculus (Brown et al., 2000; Feldheim et al., 2000; McLaughlin et al., 2003) and the projections of cortical pyramidal cells to the spinal cord (O’Leary and Terashima, 1988). Despite their prevalence throughout the CNS, comparatively little is known about how interneurons target their synaptic partners during development. This may in part be due to their vast morphological, molecular and physiological diversity (Markram et al., 2004; Somogyi and Klausberger, 2005), making their identification during development difficult because of a lack of early specific markers. In addition, the local nature of their connectivity precludes the use of tracing studies to reveal their early projection patterns.

The retina offers an attractive model to investigate how synaptic specificity is achieved by interneurons. The stereotypic organization of this structure is such that connectivity between cells is confined to two distinct synaptic

laminae, the outer and inner plexiform layers (OPL, IPL). Within the IPL, connections between specific pre- and post-synaptic partners are organized within two distinct sublaminae, each of which contains multiple strata (Mumm et al., 2005; Nelson et al., 1978; Pang et al., 2002). By monitoring how interneurons confine their arbors to specific sublaminae *in vivo*, insights into the mechanisms that determine synaptic specificity can be gained. Zebrafish, which are relatively transparent during development, are well suited for such studies (Jontes et al., 2000; Kay et al., 2004; Mumm et al., 2005). Here, taking advantage of genetic constructs that specifically label retinal amacrine cells in transgenic zebrafish, we investigate how these interneurons organize their arbors within sublaminae to target their synaptic partners *in vivo*.

Like many CNS interneurons, amacrine cells are inhibitory. Amacrine cells modulate the vertical flow of visual information from photoreceptors via bipolar cells to ganglion cells. They contact bipolar cell axons and ganglion cell dendrites in the IPL. The IPL is further sublaminated to segregate circuits that respond differentially to the onset of light. The processes of cells that hyperpolarize with increased light intensity are confined to the outer half (OFF sublamina) of the IPL, whereas processes of cells that depolarize are confined to the inner half

(ON sublamina) (Famiglietti et al., 1977; Famiglietti and Kolb, 1976; Stell et al., 1977).

Birthdating studies in diverse vertebrates suggest that ganglion cells are the first generated cell type (Hu and Easter, 1999; Prada et al., 1991; Rapaport et al., 1996; Rapaport et al., 2004). Of the neurons that contribute their processes to the IPL, the generation of ganglion cells is followed by the generation of amacrine cells and bipolar cells in overlapping sequence (Prada et al., 1991; Rapaport et al., 1996; Rapaport et al., 2004). Our own previous observations (Kay et al., 2004) and those of others (Gunhan-Agar et al., 2000; Williams et al., 2001) suggest that in the absence of ganglion cells, amacrine cell arbors stratify within ON and OFF sublaminae. Thus, despite their early generation, ganglion cells appear to be dispensable for amacrine cell stratification. With no absolute requirement for their major synaptic partners, how do amacrine cells achieve their stratification pattern? This question has remained elusive, as available immunocytochemical markers only label differentiated amacrine cells after they are stratified (Bansal et al., 2000; Gunhan et al., 2002; Reese et al., 2001; Stacy and Wong, 2003). It has therefore not been possible to determine whether amacrine cell neurites remodel within the IPL before occupying a sublamina, or whether they specifically target a sublamina, responding to cues already present in the nascent IPL.

Here, we use two different genetic constructs to drive the expression of fluorescent proteins in amacrine cells in transgenic zebrafish. By using *pancreas transcription factor 1a* (*ptf1a*) regulatory elements to drive expression of green fluorescent protein (GFP), we were able to follow the entire population of amacrine cells during development and monitor how amacrine neurites contribute to the formation of the IPL.

To determine how individual amacrine cells stratify within the IPL, we used *pax6* enhancer elements to drive the expression of fluorescent proteins in small subsets of amacrine cells. Because we followed individual cells from the time their neurites first elaborate until they stratify, we were able to gain insight into the developmental rules that govern amacrine cell stratification. Our observations provide the first view of how individual amacrine interneurons organize their processes to target specific synaptic partners within the sublaminae of the IPL. They also suggest that the strategies used by interneurons and projection neurons to achieve synaptic specificity could be diverse.

Materials and methods

Generation of the *ptf1a::GFP* transgenic line

Bacterial artificial chromosome (BAC) recombineering (Copeland et al., 2001) was used to generate six independent transgenic lines in which GFP replaced the *ptf1a* coding sequence in a genomic BAC spanning the *ptf1a* locus. All six lines displayed an identical pattern of GFP expression in the pancreas, hindbrain and retina, faithfully recapitulating the normal pattern of *ptf1a* expression (Lin et al., 2004). A detailed description of these lines will be provided in a separate publication.

Labeling individual amacrine cells in *ptf1a::GFP* retinae

Two plasmids were injected into one-cell-stage fertilized eggs from crosses of *ptf1a::GFP* fish. α -tubulin::Gal4VP16 (pTub-GVP) (Koster and Fraser, 2001) was co-injected with UAS::M-mCherry. The latter plasmid was made by cloning the 14×UASE1b promoter

(Koster and Fraser, 2001) upstream of a plasmid containing monomeric Cherry (mCherry) (Shaner et al., 2004) fused to the first 20 amino acids of zebrafish Gap43, a sequence containing palmitoylation sites (Kay et al., 2004). This results in membrane targeting of the fluorescent protein (M-mCherry).

Generation of *pax6DF4::M-CFP* and *M-YFP* transgenic lines

Seven cyan fluorescent protein (CFP) and four yellow fluorescent protein (YFP) transgenic lines of zebrafish (see Table S1 in the supplementary material) were generated by modifying a plasmid previously used to drive stable expression of membrane-targeted GFP in subpopulations of amacrine cells (Kay et al., 2004). Briefly, CFP or YFP was fused to a membrane-targeting sequence of zebrafish Gap43. Expression of the fusion protein was regulated by an *EF1 α* promoter and a hexamer of the DF4 *pax6* enhancer element. Most of the transgenic lines were generated in a wild-type background. However, three out of the four YFP founders are carriers for *roy orbison* (*roy*), a pigmentation mutant in which iridophores are reduced (Ren et al., 2002). The development and histology of the retina in *roy* fish appear indistinguishable from wild-type zebrafish (Ren et al., 2002).

Immunohistochemistry

Larval fish were fixed as described by Kay et al. (Kay et al., 2004). Cryosections (20 μ m) were incubated in 5% normal donkey serum for 1 hour, followed by an overnight incubation in mouse anti-5E11 (1:50, a gift from Dr J. M. Fadool) or mouse anti-zn5 (1:500, Zebrafish International Resource Center) diluted in 0.1 M PBS containing 0.5% Triton X-100. Following washes in PBS and incubation in Alexa Fluor 568 goat anti-mouse (Molecular Probes; 1:1000 in 0.1 M PBS) for 1 hour, sections were cover-slipped in Vectashield (Vector Laboratories). Alexa Fluor 633 Phalloidin (1:50; Molecular Probes) was sometimes included with the primary antibody.

Live imaging

Embryos were prepared for in vivo imaging as described by Kay et al. (Kay et al., 2004). A detailed protocol is also available (Lohmann et al., 2005). Confocal image stacks were acquired on an Olympus FV500 or a BioRad 1024M with water objectives, including a 60× (NA 1.1, Olympus), a 100× (NA 1.0, Olympus) and a 4× air objective (NA 0.28, Olympus). A series of optical planes encompassing the entire neuritic arbor of the cell being monitored was obtained at each time point. To follow the motility of processes, images were obtained every 5 to 10 minutes for a period of 30 minutes. For these experiments, the confocal aperture was fully open to permit the use of minimal laser power and to reduce phototoxicity. To monitor the lifetimes of amacrine cell processes, images were obtained every minute, for 30 minutes.

Counter-staining transgenic embryos with BODIPY Texas Red

To define the retinal location of amacrine cells and to delineate the boundaries of the IPL, embryos were counterstained with CellTrace BODIPY Texas Red methyl ester (Molecular Probes), a vital dye that labels cell membranes (Cooper et al., 2005). Embryos were incubated for 1 hour in 200 μ M BODIPY Texas Red in 0.3× Danieau's solution containing 1-phenyl-2-thiourea (PTU). Following several washes in 0.3× Danieau's solution, embryos were prepared for live imaging.

Image analysis

Image analysis including orthogonal rotations and 3D reconstructions were carried out using Metamorph (Universal Imaging) or Amira (TGS Template Graphics software). They were further processed in Adobe Photoshop CS.

To assess directionality of neurite elaboration by immature amacrine cells, we imaged cells at 15-30 minute intervals over 2-3

hours. Three-dimensional reconstructions of the cells were analyzed at each time point. Two lines, at 90° angles to each other, intersecting the soma at its mid-point, served to partition the surrounding area into three regions: towards the outer limiting membrane (OLM), the ganglion cell layer (GCL) and sideways (S). We scored neurite tips as being oriented toward the OLM, GCL or sideways according to their localization within one of these areas.

To measure changes in neurite length, the distance between the tip of a process and its branch point or its point of origin on the cell body was measured using the *xyz* function of Metamorph. This measurement function takes into account the *xy* pixel size and the *z*-distance between optical planes.

Time-lapse images of isolated amacrine cells in the context of the developing IPL were acquired approximately every 2 hours starting at day 3, around 54 hours post-fertilization (hpf), and continued until day 4. Synaptogenesis between amacrine and ganglion cells in the IPL commences at around 60 hpf (Schmitt and Dowling, 1999). By the third day postfertilization (dpf), all cell and plexiform layers are present. The first electroretinographic responses and optokinetic reflexes are recorded around 4 dpf (Easter and Nicola, 1996; Schmitt and Dowling, 1999). The densely labeled CFP⁺ plexus between the inner nuclear layer (INL) and ganglion cell layer (GCL) in [TG(*pax6-DF4::M-CFP*)^{Q01}] provided the boundaries of the IPL. At later time points, the demarcation between this plexus and cells in the INL and GCL is definitive. Early in development, however, cells (likely displaced amacrine cells) are found embedded within the plexus, giving it a discontinuous appearance. At these stages the outer-most and inner-most regions, where a continuous plexus was apparent, were defined as the IPL boundaries.

To examine the distribution of processes of isolated amacrine cells (GFP⁺ or YFP⁺) in relation to the depth of the IPL (CFP⁺), we selected three image planes that excluded the cell body and rotated them orthogonally using Metamorph. At the orthogonal plane, a threshold was applied to the images. The IPL was divided into two equal halves, an outer (INL side, 'OFF') and an inner (GCL side, 'ON') sublamina. GFP or YFP pixel intensity within each sublamina was measured and averaged for the three image planes.

Results

An amacrine neurite plexus emerges between two amacrine cell populations

To examine how amacrine neurites contribute to the formation of the IPL, we examined the retinae of *ptfla::GFP* transgenic zebrafish. At 76 hpf, retinal GFP expression is restricted to horizontal cells in the outer retina and populations of amacrine cells in the inner retina. Two populations of GFP⁺ amacrine cells were identified, one was located within the INL and another population, with comparatively fewer cells, was found displaced to the GCL (Fig. 1A). The identity of both populations as amacrine cells was confirmed by their immunoreactivity for the 5E11 antigen, a marker of amacrine cells (Fig. 1A) (Fadool et al., 1999; Link et al., 2000). In addition, GFP⁺ cells in the GCL did not have detectable axons, suggesting that they were not ganglion cells. At this stage, a laminated GFP⁺ plexus was detected intervening between the two amacrine cell populations (Fig. 1A).

To examine how amacrine cells become displaced to the GCL and how the GFP⁺ plexus emerges during development, we imaged the retinae of *ptfla::GFP* transgenic fish in vivo and counterstained the embryos with BODIPY Texas Red to visualize the general structure of the retina (Cooper et al., 2005). At early time points, many GFP⁺ cells were detected two to three cell bodies away from the ILM, overlying the GFP⁻

somata of ganglion cells (Fig. 1B,C, see Fig. S1 in the supplementary material). Two morphologically distinct GFP⁺ somata could be distinguished. The vast majority of cells had elongated somata, whereas a smaller number of vitreally located cells had rounded or flattened somata (Fig. 1B,C). Time-lapse imaging of individual, vitreally located amacrine cells clearly revealed the orientation of their neurites towards the GFP⁺ amacrine cells in the INL from very early time points (Fig. 1B, see Fig. S2 in the supplementary material). Starting around 42 hpf, a GFP⁺ plexus emerged between the two amacrine cell populations and, with time, the vitreally located cells became displaced towards the GCL (Fig. 1C). Although higher resolution confocal imaging revealed some GFP⁺ neurites extending towards the GCL (see Movie 1 in the supplementary material), the overwhelming majority of GFP⁺ neurites was confined to the neuropil between the two populations of amacrine cells. Thus, amacrine cells located in the INL and displaced amacrine cells orient their neurites towards each other from the outset. With time, the GFP⁺ amacrine neurite plexus transforms from an apparently diffuse plexus at 51 hpf (Fig. 1C) to a laminated plexus by 76 hpf (Fig. 1A). How the neuritic arbors of individual amacrine cells transform during this time could not be gauged in *ptfla::GFP* transgenic fish because of the high density of labeling. We therefore sought alternative means to label individual amacrine cells.

Amacrine cell-specific transgenic lines expressing different color fluorescent proteins

We previously used the *pax6* enhancer element (*pax6-DF4*) to generate stable transgenic lines (lines 220, 244 and 243) expressing membrane-targeted GFP in subpopulations of amacrine cells (Kay et al., 2004). The neurites of the GFP-labeled amacrine cells ramify in two prominent sublaminae within the IPL. Co-labeling of these GFP⁺ sublaminae with immunoreactivity for choline acetyltransferase, suggested they correspond to OFF and ON sublaminae (Kay et al., 2004; Yazulla and Studholme, 2001). Variable levels of expression were seen between these lines most likely caused by integration site effects, such that a high density of GFP expression in some lines (line 220) made it difficult to distinguish between the neuritic arbors of individual cells, whereas in other lines (lines 244 and 243) fewer amacrine cells were labeled (Kay et al., 2004).

To follow the behavior of individual amacrine cells, we took advantage of the variegated patterns of expression of the *pax6-DF4* construct to generate stable transgenic lines expressing membrane-targeted CFP or YFP. Seven CFP [TG(*pax6-DF4::M-CFP*)] and four YFP [TG(*pax6-DF4::M-YFP*)] transgenic lines were generated (see Table S1 in the supplementary material). For simplicity, these lines are referred to by their allelic designation. Thus, the first generated transgenic line [TG(*pax6-DF4::M-CFP*)^{Q01}] is referred to as line Q01. In most of the lines (eight out of 11), fluorescent protein expression was confined to the retina (Fig. 2A,C), similar to the original GFP lines. As expected, some lines exhibited sparse labeling (e.g. lines Q08, Q11, Q14) and were exploited to follow the behavior of individual amacrine cells (Fig. 2B,D). However, as the number of cells labeled in an individual embryo varied, on average >20 animals had to be screened to obtain embryos with such isolated cells. In all the retina-specific transgenic lines, fluorescent protein expression in the retina was first apparent in

neuroblasts by 24 hpf. Starting on the second day and persisting into adulthood, expression became confined to amacrine cells, with somata in the inner nuclear layer (INL) and neurites ramifying in the IPL (Fig. 2B,D).

In three lines, CFP expression was ubiquitous (e.g. line Q01; Fig. 2E). These lines proved useful as a tool to visualize the general organization of the developing retina. The membrane targeting of CFP resulted in the neuropil-rich plexiform layers being densely labeled, and the soma-rich nuclear layers only outlined (Fig. 2F). By crossing ubiquitously expressing CFP fish with amacrine-specific GFP or YFP lines, we were able to monitor the behavior of individual amacrine cells at defined locations within the retina.

Early amacrine cells show undirected process outgrowth

We imaged embryos as early as 41 hpf to capture the behavior

of amacrine cells prior to their arrival at the interface with the nascent IPL. During migration, amacrine cell processes did not appear to be polarized towards their eventual target, the IPL ($n=5$ cells). Instead, they had multiple processes emerging from their cell body that were highly dynamic (Fig. 3). Extensive process outgrowth from amacrine cells thus occurs well before these cells reach their final somal positions.

Even when amacrine cells were detected near the border of the IPL and the forming INL, they continued to elaborate processes that appeared to sample the environment (Fig. 4A). This stage of exuberant outgrowth lasted for several hours, and cells displaying this behavior were detected as late as 63 hpf (Fig. 4A, see also Movie 2 in the supplementary material). Some of these early processes were branched, whereas others were simple extensions. However, despite this apparently random sampling behavior, a greater number of amacrine processes (per cell) were directed towards the GCL when compared with other directions (Fig. 4B-D, see Movie 3 in the supplementary material).

Amacrine cells polarize by the relative stabilization of GCL-directed processes

Given the multipolar exploration exhibited by these processes, we next asked whether amacrine neurites extending towards or away from the

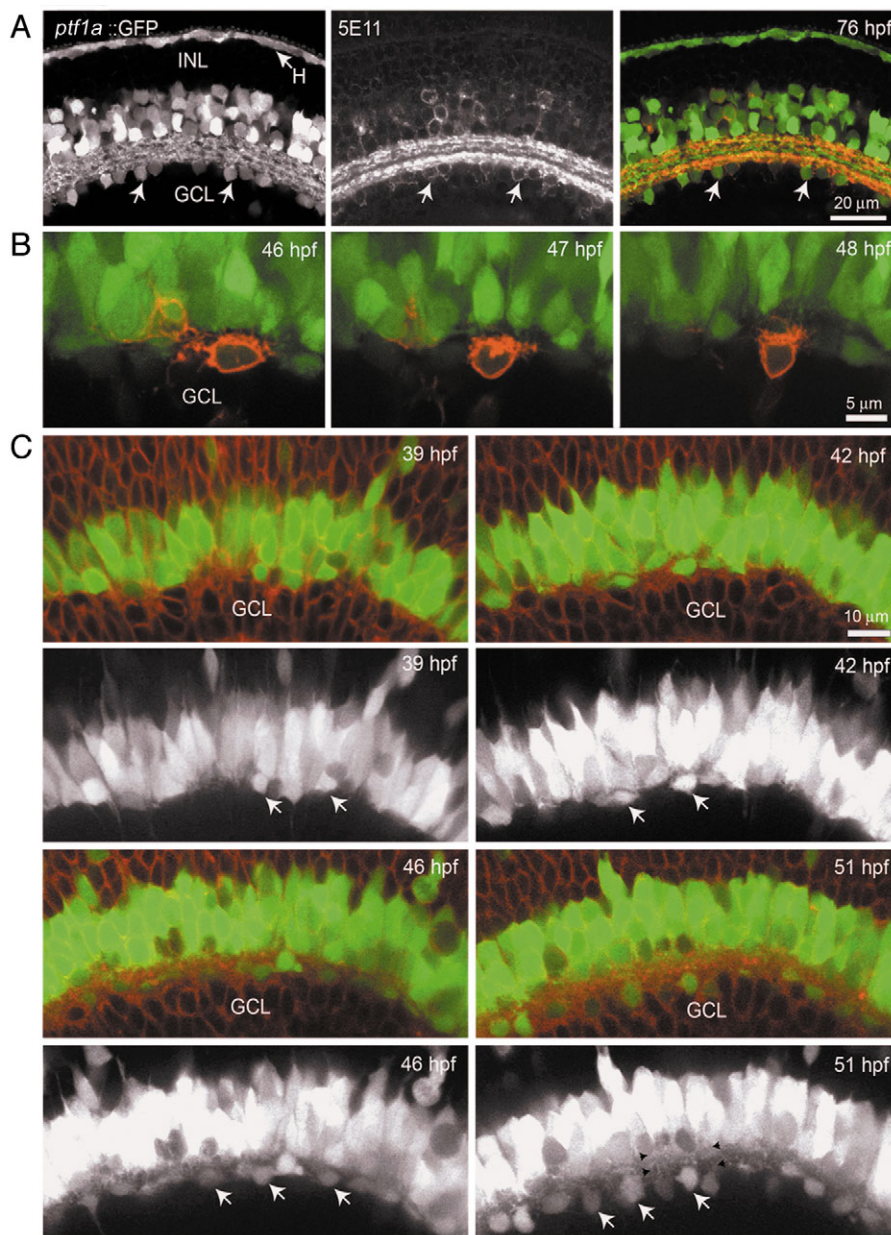


Fig. 1. *ptf1a* regulatory elements drive expression of GFP in amacrine cells in transgenic zebrafish. (A) Confocal images of a cryosectioned retina from a *ptf1a::GFP* fish at 76 hpf reveal a population of GFP⁺ cells in the inner portion of the INL and a population of cells in the GCL that are immunoreactive for the 5E11 antigen, suggesting they are amacrine cells (arrows in the GCL indicate displaced amacrine cells). The arbors of both amacrine cell populations ramify in the IPL, forming a laminated plexus. Horizontal cells (H) located in the outer part of the INL also express GFP. (B) In vivo confocal time-lapse images of a vitreally located GFP⁺ amacrine cell co-labeled with membrane-targeted mCherry (red) driven by an α -tubulin promoter reveal that its neurites are oriented towards the INL. (C) In vivo confocal time-lapse images reveal that both populations of GFP⁺ amacrine cells (green) can be identified as early as 39 hpf. The vitreally located GFP⁺ cells with rounded or flattened somata (arrows) become displaced to the GCL as a plexus forms (black arrowheads, 51 hpf) between them and the INL population of GFP⁺ amacrine cells (46 and 51 hpf). Counterstaining with BODIPY Texas Red demonstrates that the GFP⁺ plexus lies within the forming IPL. Gray-scale images of GFP⁺ amacrine cells are shown to permit better visualization of GFP⁺ processes.

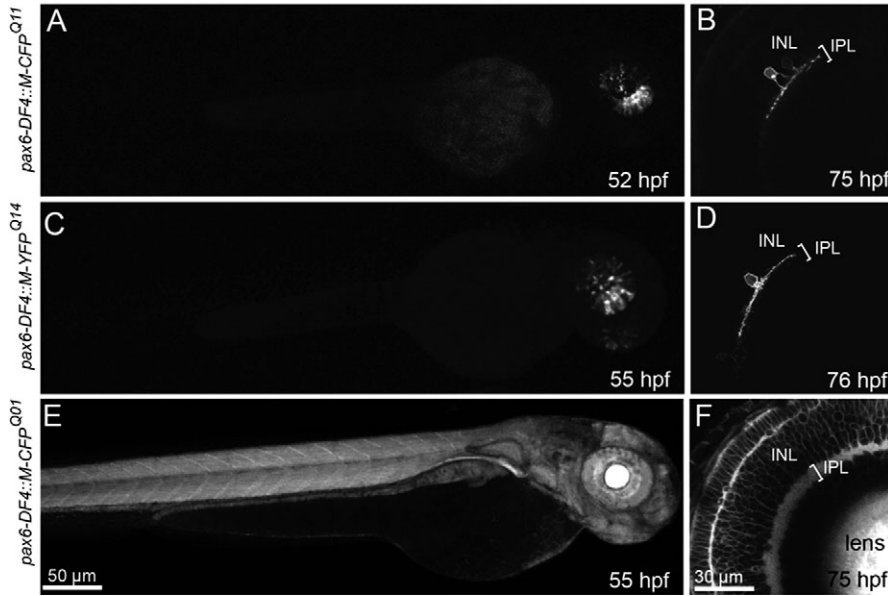


Fig. 2. The *pax6-DF4* enhancer element drives expression of fluorescent proteins in transgenic lines of zebrafish. In most of the lines generated, expression of membrane-targeted fluorescent proteins was confined to the retina (A-D). Confocal images of larval zebrafish from CFP line Q11 (A) and YFP line Q14 (C) reveal that at early stages, expression within the retina is in clones of cells that span the neuroepithelium. With time, expression becomes confined to amacrine cells located in the INL with processes ramifying in the IPL. The number of labeled amacrine cells varied, but was sometimes sparse enough to allow individual amacrine cells to be visualized unambiguously (B,D). Ubiquitous expression throughout the embryo was observed in CFP line Q01 (E). In the retina of line Q01, cells in the nuclear layers were outlined and the plexiform layers appeared to be densely labeled (F).

GCL differed in their dynamic behavior in a manner that could explain the eventual formation of a polarized arbor. We performed quantitative analysis of time-lapse recordings of individual amacrine cell processes to address this question. Imaging more frequently (inter-frame intervals of 5-10 minutes; $n=9$ cells) revealed that both OLM-directed ($n=27$

processes) and GCL-directed ($n=25$ processes) processes underwent rapid remodeling with similar extension and retraction rates (Fig. 5A-C) that reached a maximum motility rate of $0.96 \mu\text{m}/\text{minute}$. However, although the overall growth and retraction rates were similar (Fig. 5C), we found a significant difference between the life times of OLM-directed ($n=15$ processes) and GCL-directed processes ($n=17$ processes; 6 cells; Fig. 5D). Of the GCL-directed processes, 65% persisted for the entire period of recording (30 minutes), in contrast to only 33% of the OLM-directed processes (Fig. 5D, $P<0.001$, Mann-Whitney rank sum test).

Lateral territories of developing amacrine cell arbors in the IPL undergo remodeling

With development, amacrine cells eventually project their neurites exclusively towards the GCL, arborizing laterally within the forming IPL. Our time-lapse recordings revealed that another phase of dynamic remodeling ensues, resulting in an arbor that demarcates the cell's lateral territory. Analysis of motility showed that amacrine cell processes within the IPL reached maximum growth rates of $0.59 \mu\text{m}/\text{minute}$, with similar extension and retraction rates ($n=3$ cells, 24 processes; Fig. 6A-C). Interestingly, the motility rates of processes extending and retracting within the IPL are not significantly different to the processes of less mature amacrine cells ($P>0.05$, Mann-Whitney rank sum test). Changes in the territory of the lateral arbor did not simply result from continuous growth. Rather, dynamic remodeling, retraction, extension and the de novo formation of branches, resulted in shifts of the territory occupied by the lateral arbor within the IPL (Fig. 6D,E; see Movie 4 in the supplementary material).

Amacrine cells recognize sublamina-specific cues in the forming IPL

We next asked what mechanisms amacrine cells use to restrict their arbors to a particular sublamina within the IPL. Many of the *pax6* transgenic lines we generated have a greater number of amacrine cells stratifying in the OFF sublamina than in the ON sublamina of the IPL at maturity. Thus, most of our

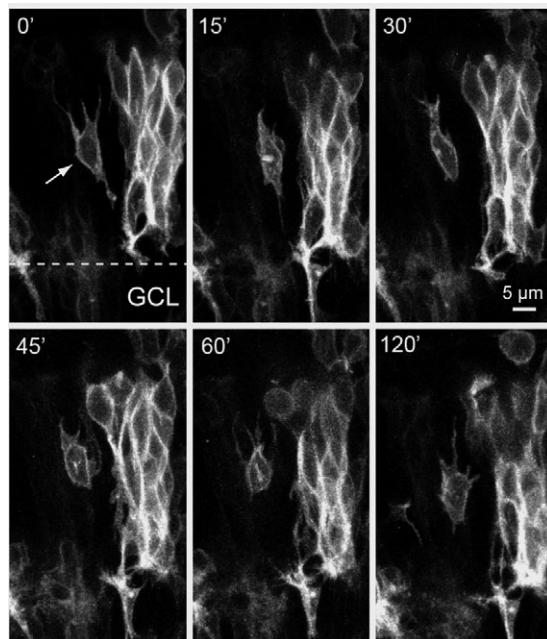


Fig. 3. Migrating amacrine cells show undirected neurite outgrowth. Time-lapse images of a YFP⁺ amacrine cell (arrow) in line Q14 migrating towards the GCL. Multiple neurites emerge from the amacrine cell, but they do not appear to be polarized towards the GCL. Imaging commenced at 51 hpf (0'). The dashed line represents the position of the future IPL, at the interface between the forming INL and GCL. Clones of FP-expressing cells (like those to the right of the migrating amacrine cell) are usually seen in the *pax6* transgenic lines at early stages of development.

observations are restricted to amacrine cells that stratify in the outer sublamina of the IPL. We followed individual GFP⁺ or YFP⁺ amacrine cells ($n=18$ cells) from the time they first extended lateral arbors within the IPL (demarcated by the ubiquitous membrane labeling of CFP line Q01) until they had established monostratified arbors between 70-73 hpf, when sublamination is evident (Kay et al., 2004). From the earliest time points, the neuritic arbors of all cells followed were heavily biased to the outer half of the IPL, where they would ultimately stratify (see examples in Fig. 7A,B). Morphometric analysis was used to quantify this bias. We divided the depth of the IPL into an outer and an inner half, and measured the contribution of amacrine neurite-derived fluorescence to each

half at two time-points, early (57-62 hpf) and at maturity (70-72 hpf). We found an overwhelmingly high percentage of neurite-derived fluorescence in the outer half of the IPL at both time points (99.4% at 57-62 hpf and 98.4% at 70-72 hpf, $n=10$ cells; Fig. 7C). This bias was maintained despite growth in the thickness of the IPL over time (from 10 μm at 57-59 hpf to 14.5 μm at 70-71 hpf, averaged across five retinæ) and lateral expansion of the neuritic arbors.

To exclude the possibility that an early exuberance within the IPL was undetected, we used time-lapse observations to follow amacrine cells as they were docking at the IPL (Fig. 7B). Amacrine neurites were confined to the outer half of the IPL, never displaying diffuse growth throughout the depth of the IPL (Fig. 7B). This suggests that even at their first contact with the nascent IPL, amacrine cell processes recognize sublamination cues.

The mechanisms of neurite elaboration into OFF and ON IPL sublaminae could differ. Although we found an early bias of OFF amacrine cells for the outer IPL, it is the first sublamina that amacrine cell neurites encounter by virtue of their somal position in the INL. This left open the possibility that stratification in the inner half of the IPL (ON sublamina) required exuberant growth. We managed to observe a small number of amacrine cells that eventually stratified in the ON sublamina ($n=8$ cells). We monitored GFP⁺ cells in the background of the ubiquitously-expressing CFP line Q01 (Fig. 8A) or CFP⁺ cells in the background of a larger population of GFP⁺ amacrine cells (line 220) known to stratify in OFF and ON sublaminae (Fig. 8B) (Kay et al., 2004). For these cells, no exuberance into outer, and thus 'inappropriate', IPL sublaminae was observed, even at early time points (52-58 hpf). Instead, the immature neurites appear to directly grow towards the inner half of the IPL and spread laterally upon reaching their appropriate lamina (Fig. 8A,B).

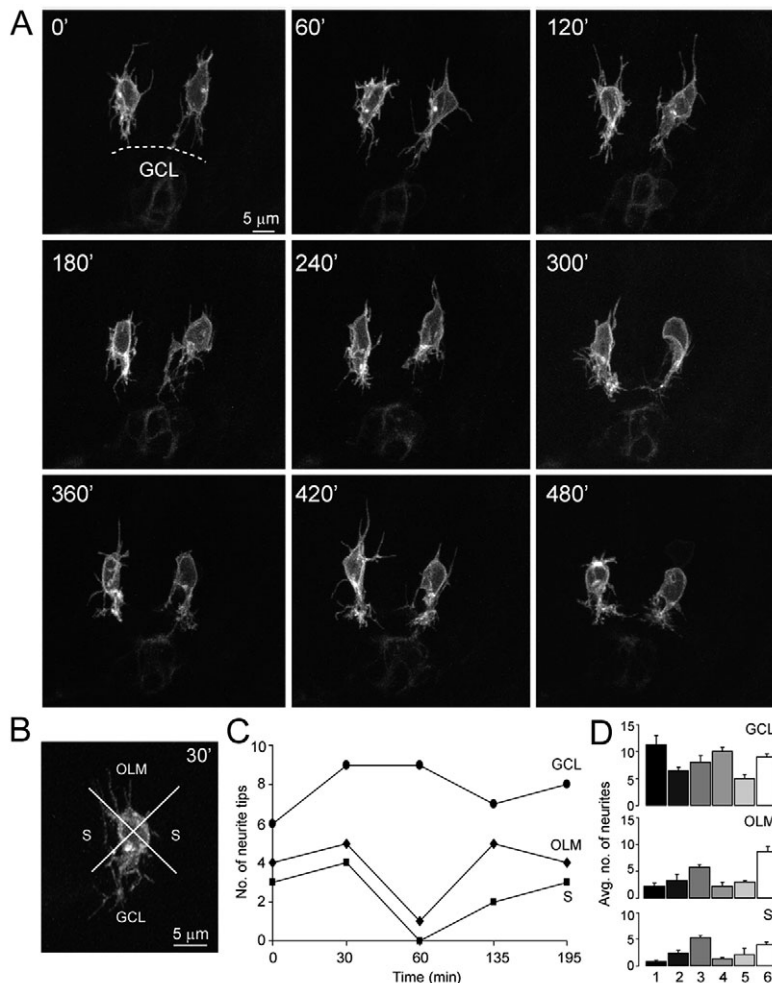


Fig. 4. Exuberant neurite outgrowth continues even when amacrine cells are located near or at their final somal positions. (A) Time-lapse confocal images of a pair of CFP⁺ amacrine cells from line Q11 reveal neurites directed appropriately towards the GCL, and erroneously towards the outer retina. Imaging commenced at 56 hpf (0') and proceeded to 64 hpf (480'). To examine whether the neurite extension of amacrine cells located near their final somal positions displayed directionality, we scored neurites as being directed towards the GCL, the OLM or sideways (S), as shown for the amacrine cell in B. For the cell in B, during the period of recording, the number of neurite tips directed towards the GCL was consistently found to exceed the number of neurite tips directed elsewhere (C). (D) Histograms of a similar analysis for six cells (each differently shaded), where the number of neurites was averaged over a period of 90 minutes.

Discussion

Diverse strategies used by projection neurons and interneurons to target synaptic partners

We took advantage of the stereotypic organization of circuitry in the retinal IPL to investigate how amacrine interneurons achieve their laminar specificity and thereby target specific synaptic partners during development. Our ability to label these cells early and examine their development in vivo provides the first insights into the cellular mechanisms used by amacrine cells to achieve synaptic specificity. Our recordings of individual amacrine cells in the zebrafish retina clearly demonstrate that once the processes of amacrine cells reach the forming synaptic neuropil of the IPL, their arbors lateralize preferentially within the appropriate sublamina. These findings demonstrate that the targeting of amacrine cell neurites is highly directed and does not involve extensive laminar remodeling. This is in contrast to the way in which

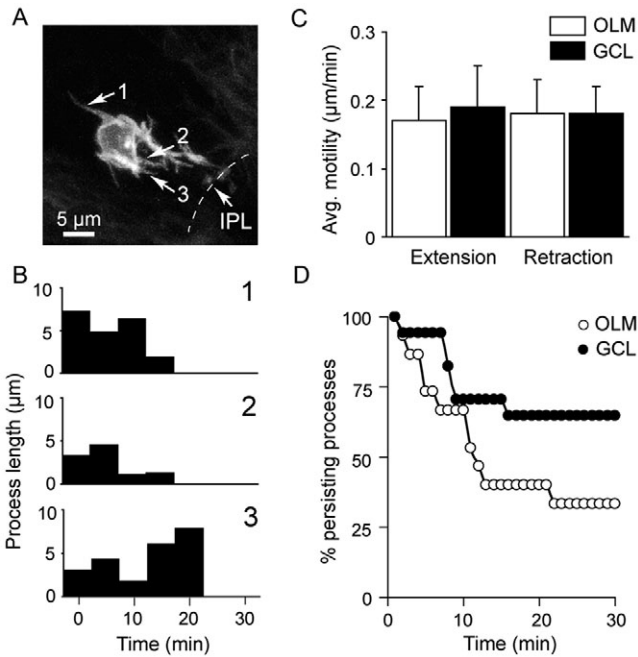


Fig. 5. Amacrine neurites directed towards the GCL or the OLM show similar motility rates but significantly different life times. (A) Changes in neurite length for an OLM-directed process (1) and GCL-directed processes (2,3) of an amacrine cell (CFP⁺ line Q11, 54 hpf) over a period of 30 minutes are plotted in B. Such measurements were used to calculate average motility rates (C). Average extension rates for processes directed towards the OLM were found to be $0.17 \pm 0.05 \mu\text{m}/\text{minute}$, and toward the GCL $0.19 \pm 0.06 \mu\text{m}/\text{minute}$. Average retraction rates from the OLM were found to be $0.18 \pm 0.05 \mu\text{m}/\text{minute}$ and from the GCL $0.18 \pm 0.04 \mu\text{m}/\text{minute}$. These rates were not significantly different ($n=9$ cells; 8–19 processes per group; $P>0.05$ for all groups, Mann-Whitney rank sum test). (D) A significant difference was found between the life times of processes directed towards the GCL ($n=17$ processes) and the OLM ($n=15$ processes; $P<0.001$, Mann-Whitney rank sum test).

the dendrites of retinal ganglion cells, the major post-synaptic partners of amacrine cells, are believed to achieve their mature stratification in the IPL. Early in development, ganglion cell dendrites appear to ramify through the entire depth of the IPL in mammals (Bodnarenko et al., 1995; Maslim and Stone, 1988). Extensive reorganization, including the retraction of inappropriately placed dendrites, is suggested to lead to their mature stratification pattern (Chalupa and Gunhan, 2004; Maslim and Stone, 1988). In the light of the findings here, it will be of interest to determine whether non-mammalian ganglion cells undergo extensive dendritic remodeling as well.

The directed targeting of amacrine neurites to appropriate sublaminae in the IPL is similar to the exquisite lamina-specific outgrowth suggested for layer 4 cortical interneurons (Callaway and Katz, 1992). Intracellular staining of these spiny stellate interneurons in brain slices revealed lamina-specific axonal projections to layers 2/3, 5 and 6, where their post-synaptic partners reside, even early in development. Such specificity has also been suggested for the manner in which retinal ganglion cell axons target sublaminae in the chick optic tectum (Yamagata and Sanes, 1995), or form retinotopic maps in the zebrafish tectum (Stuermer, 1988). However, these

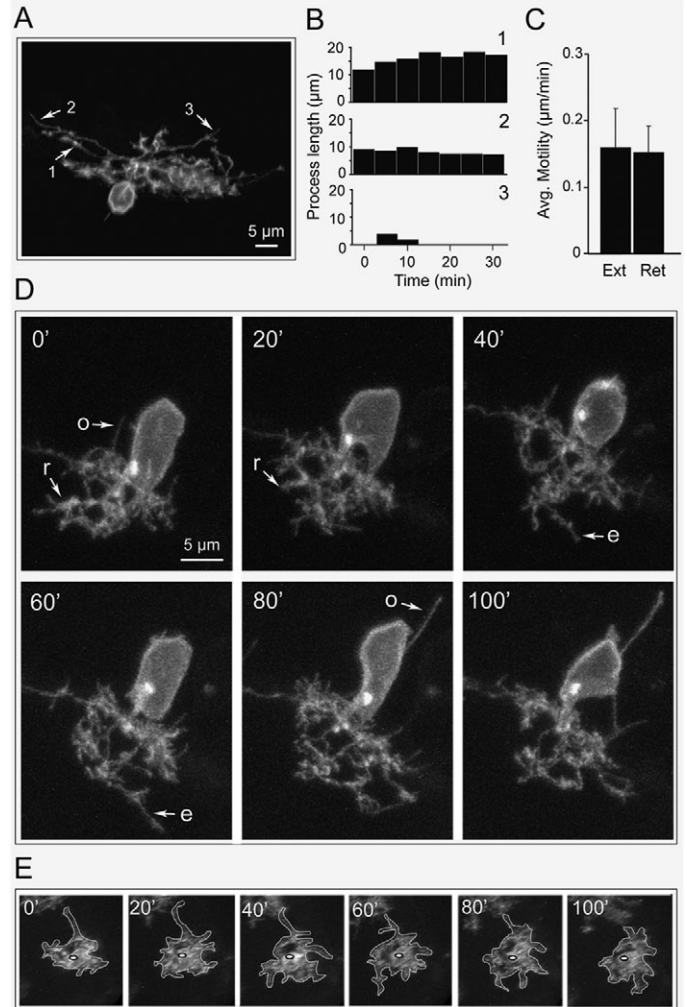


Fig. 6. Analysis of the dynamic behavior of amacrine neurites within the IPL reveals extensive remodeling. Changes in neurite length over a period of 30 minutes were measured for amacrine cells with extensive lateral arbors in the IPL and used to calculate average motility rates. (A) Changes in length for three neurites (1,2,3) from the lateral arbor of an amacrine cell (CFP⁺ line Q11, 58 hpf) are plotted in B. (C) Average extension and retraction rates of processes within the IPL were found to be similar ($0.16 \pm 0.06 \mu\text{m}/\text{minute}$ and $0.15 \pm 0.04 \mu\text{m}/\text{minute}$, respectively; $n=3$ cells, 24 processes; $P>0.05$; Mann-Whitney rank sum test). (D) Time-lapse images of an amacrine cell (54 hpf at 0') digitally rotated to provide a clearer view of its lateral arbor. Extensions (e) and retractions (r) of neurites within the IPL resulted in dramatic changes of the territory occupied by the lateral arbor (see E). Occasionally, neurite outgrowth towards the outer retina, from the lateral arbor (o at 0') or from the cell body (o at 80') was observed. (E) Time-lapse images of the amacrine cell in D digitally rotated to provide en face views of the lateral arbor. The extent of the cell's lateral territory is outlined in white and the location of the presumed Golgi (bright spot in the cell body in D) is depicted by a black oval.

examples contrast with the extensive remodeling reported for the axonal arbors of most other projection neurons, including those of the corticospinal tract (Luo and O'Leary, 2005). It therefore appears that the two major classes of neurons, interneurons and projection neurons, may employ diverse strategies to target their synaptic partners.

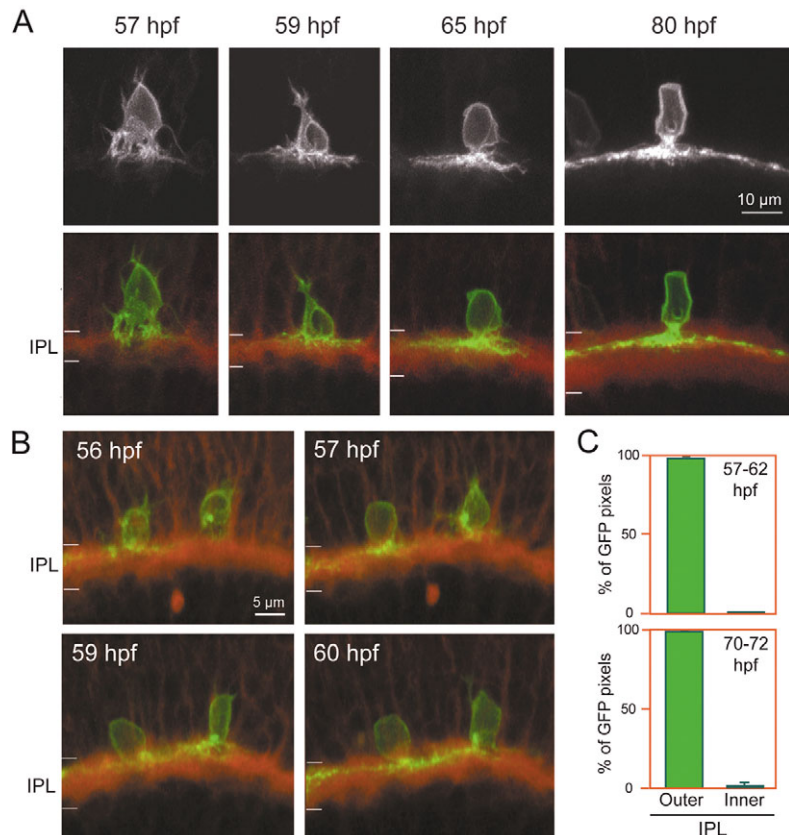


Fig. 7. Amacrine cells that ultimately stratify in the OFF sublamina display an early bias for the outer half of the IPL. (A) Confocal time-lapse images of a YFP⁺ amacrine cell from line Q08 (green) in the background of the ubiquitously-expressing CFP line Q01 (red). The amacrine cell confines its lateral arbors to the outer part of the IPL from the earliest time points (57 hpf) until the time when it is stratified (80 hpf). (B) Early restriction of neurites to the outer half of the IPL for OFF amacrine cells can be better appreciated for a cell (GFP line 244, green) that arrives at the interface of the IPL (right cell in all panels) demarcated by the ubiquitous expression of CFP (line Q01, red). (C) Morphometric analysis of 10 GFP⁺ or YFP⁺ cells imaged in the background of line Q01 confirmed that the vast majority of GFP⁺ or YFP⁺ pixels lies in the outer half of the IPL early (57-62 hpf) and late (70-72 hpf), for presumed OFF amacrine cells.

presence of sublamina-specific cues. We think that direct cell-cell interactions, rather than molecular gradients, are the more likely candidates for such cues. This is because, compared with other CNS regions in which molecular gradients set up specific axonal arborization patterns (e.g. the tectum or superior colliculus), the IPL is relatively thin and compact. In the superior colliculus, for example, ephrin gradients extend over several millimeters along the anteroposterior and mediolateral axes to help create retinotopic maps (Brown et al., 2000; Feldheim et al., 2000; O'Leary and McLaughlin, 2005). In the IPL, such molecular gradients would

need to be very steep to set up not only the ON and OFF sublaminae, but also the multiple strata that lie within each sublamina, as they are only micrometers apart (Wassle and Boycott, 1991; Werblin et al., 2001).

Cellular behaviors and mechanisms directing amacrine cell lamination

In order for amacrine interneurons to appropriately target their synaptic partners, they need to migrate towards the GCL and then localize their arbors to a specific sublamina in the IPL. Our *in vivo* observations suggest that migrating amacrine cells extend and retract multiple processes, appearing to search for cues as they navigate towards the GCL. Presumptive amacrine cells with such morphologies have been described in serial electron microscopy (Hinds and Hinds, 1978; Hinds and Hinds, 1983) and Golgi (Prada et al., 1987; Quesada et al., 1981) studies of mouse and chick retina. This migratory mode adopted by amacrine cells appears to be similar to that reported for migrating interneurons in the neocortex, where cells have multiple branched processes (Ang et al., 2003; Nadarajah et al., 2003). In addition, it appears to be distinct from the migratory mechanisms used by pyramidal neurons, the projection neurons of the neocortex, which include somal translocation and glial-guided migration (Nadarajah et al., 2001). Together, these observations suggest a common mode of migration for interneurons.

The environment around amacrine cells appears to be uniformly permissive for neurite outgrowth. We found that neurites can extend from their cell bodies in any direction for a protracted period even after their somata have reached the forming INL. However, amacrine neurites directed towards the GCL appear to encounter cues that encourage further elaboration within the IPL; these processes persist for longer periods than neurites directed elsewhere.

The selective elaboration of amacrine neurites within appropriate ON or OFF sublaminae in the IPL suggests the

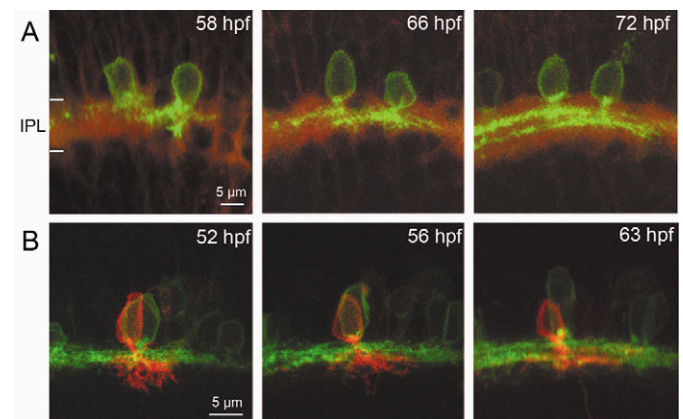


Fig. 8. Amacrine cells display an early bias for the IPL sublamina in which they will ultimately stratify. (A) Confocal time-lapse images of a pair of GFP⁺ amacrine cells from line 220 (green) in the background of the ubiquitously-expressing CFP line Q01 (red). The cell that eventually stratifies in the ON sublamina of the IPL (cell to the right) ramifies its neurites in the inner half from the outset. Similarly, the cell that eventually stratifies in the OFF sublamina (cell to the left) restricts its neurites to the outer half of the IPL from the outset. (B) Time-lapse of a CFP⁺ amacrine cell (line Q11, red) in the background of GFP line 220 (green) in which populations of OFF and ON amacrine cells are labeled.

Adhesion molecules are attractive candidates for permitting cellular interactions that could lead to the sublamina-specific targeting of amacrine cell neurites. Two members of the immunoglobulin superfamily of adhesion molecules, sidekick 1 and 2 (Sdk1 and 2), have been shown to be differentially expressed in the ON and OFF sublaminae of the chick IPL (Yamagata et al., 2002). Sdk1, expressed in the ON sublamina, has been implicated in establishing connections between ganglion, amacrine and bipolar cells that co-stratify in this sublamina, whereas Sdk2 has been implicated in establishing connectivity in the OFF sublamina. The restricted expression of cadherins within the IPL is also suggestive of their role in establishing synaptic specificity (Honjo et al., 2000; Wohrn et al., 1998). For such adhesion molecules to mediate the specific targeting of amacrine neurites to appropriate sublaminae, they would have to be expressed on the dendrites of ganglion cells or by previously arrived amacrine cells, as these two cell-types are the sole contributors of processes to the early IPL (Schmitt and Dowling, 1999). Bipolar and Müller glial cells, the two other cell types whose processes lie in the IPL, differentiate later (Peterson et al., 2001; Schmitt and Dowling, 1999); they are therefore unlikely to provide initial laminar cues but may still mediate amacrine cell stratification at later stages.

As a result of the sequence in which neurogenesis proceeds in the retina, the earliest population of differentiated amacrine cells arrives at the interface of an already formed GCL (see Fig. S1 in the supplementary material). Although ganglion cells do not appear to be essential for the stratification of amacrine cells within the ON and OFF sublaminae (Gunhan-Agar et al., 2000; Kay et al., 2004; Williams et al., 2001), an early role for ganglion cells in the orientation of amacrine neurite outgrowth towards the nascent IPL cannot be ruled out (Kay et al., 2004). The early presence of ganglion cells permits potential contact between their dendrites and the amacrine processes. These interactions could help to localize the elaboration of amacrine cell arbors to the nascent IPL.

An alternative substrate for the initial targeting of amacrine neurites could be displaced amacrine cells. Previous observations from electron microscopy and Golgi studies of chick, mouse and zebrafish retina suggest that amacrine cells become displaced by migrating through an already formed IPL to the GCL (Galvez et al., 1977; Hinds and Hinds, 1983; Schmitt and Dowling, 1999). By contrast, our recordings of *ptfla::GFP* fish suggest that displaced amacrine cells and 'normally placed' amacrine cells are present concurrently. The two populations of amacrine cell somata separate by the emergence of neurites from both populations that are oriented towards each other. Displaced amacrine cells could thus be a suitable or transient substrate for targeting by the neurites of 'normally placed' amacrine cells, a role not previously suspected.

Whether by interaction with ganglion cells or displaced amacrine cells, the earliest 'normally placed' amacrine cells form arbors that may be used by subsequent amacrine cells as scaffolds for stratification. Co-stratification of newly arriving amacrine cells with previously formed amacrine arbors may result from their common expression of adhesion molecules. Amacrine cells with a different complement of adhesion molecules would not be able to co-stratify with the earliest lamina, but could instead form new laminae either below or above the earliest strata. In this model, genetically programmed

intrinsic cues would enable amacrine cells to make different laminar choices. Another possibility is that sublaminae emerge sequentially. A report of the progressive appearance of axonin 1 immunoreactive amacrine strata in the OFF sublamina before the ON sublamina is suggestive of such a sequence (Drenhaus et al., 2004). Such a sequence may be dictated by the timing of cell birth; cohorts of amacrine cells born within a particular time window contribute neurites to a common stratum, and later-generated cohorts establish new strata. In this scenario, amacrine cells that project to a common sublamina would share common birth dates. However, birth-dating studies conducted so far suggest that this is unlikely. Although there is a general sequence in which the different neurochemical subtypes of amacrine cells are generated [gamma-aminobutyric acid (GABA)-expressing amacrine cells are generated earlier than cholinergic and dopaminergic amacrine cells (Evans and Battelle, 1987; Lee et al., 1999; Reese and Colello, 1992; Zhang and Yeh, 1990)], more than one neurochemical type of amacrine cell innervates a particular sublamina (Drenhaus et al., 2004).

Finally, amacrine cells may not only provide laminar cues for each other, but also for other retinal neurons. The finding that some classes of amacrine cells stratify before ganglion cell dendrites (Bansal et al., 2000; Gunhan et al., 2002; Reese et al., 2001; Stacy and Wong, 2003) suggests that they might provide lamination cues for ganglion cells. Although the proper stratification of bipolar cell axon terminals after pharmacological ablation of amacrine cells was taken to suggest that amacrine cells do not instruct bipolar cell stratification, only cholinergic amacrine cells were ablated in this study (Gunhan et al., 2002). This leaves open the possibility that other amacrine cells provide laminar cues for bipolar cell stratification. Our previous findings in *lakritz*, a zebrafish mutant in which ganglion cells are never generated, lend strong support to the possibility that amacrine cells instruct bipolar cell stratification. Amacrine cell sublaminae form properly in this mutant, except for in some focal regions. Bipolar cells stratify appropriately except in those local regions where amacrine cell stratification is perturbed (Kay et al., 2004). Thus, amacrine cells may be the primary organizers of sublamination in the IPL. Indeed, it raises the possibility that interneurons throughout the CNS may play central roles in the organization of circuitry. Such a role has been proposed for a population of GABAergic interneurons and Cajal-Retzius cells in the hippocampus, which, by virtue of their early arborization, guide the targeted ingrowth of afferents from other hippocampal areas (Super et al., 1998). In contrast to these hippocampal interneurons however, amacrine cells are not a transient population that exist only to serve as guides. Time-lapse studies in which amacrine cells and their synaptic partners are simultaneously visualized would help to clarify their primary role in synaptic targeting within the IPL.

This work was supported by an NIH NRSA fellowship to J.S.M., by NIH grants DK61215 and DK067210 to S.D.L., and by NIH grant EY14358 to R.O.L.W. We thank Tobias Roeser and Herwig Baier for providing the *pax6* construct, Reinhard Köster for the pTub-GVP and 14×UASE1b plasmids, and Roger Tsien for mCherry. We also thank Herwig Baier and Thomas Misgeld for critical reading of an earlier version of this manuscript, and Stephen Eglen for statistical advice.

Supplementary material

Supplementary material for this article is available at <http://dev.biologists.org/cgi/content/full/132/22/5069/DC1>

References

- Ang, E. S., Jr, Haydar, T. F., Gluncic, V. and Rakic, P. (2003). Four-dimensional migratory coordinates of GABAergic interneurons in the developing mouse cortex. *J. Neurosci.* **23**, 5805-5815.
- Bansal, A., Singer, J. H., Hwang, B. J., Xu, W., Beaudet, A. and Feller, M. B. (2000). Mice lacking specific nicotinic acetylcholine receptor subunits exhibit dramatically altered spontaneous activity patterns and reveal a limited role for retinal waves in forming ON and OFF circuits in the inner retina. *J. Neurosci.* **20**, 7672-7681.
- Bodnarenko, S. R., Jeyarasasingam, G. and Chalupa, L. M. (1995). Development and regulation of dendritic stratification in retinal ganglion cells by glutamate-mediated afferent activity. *J. Neurosci.* **15**, 7037-7045.
- Brown, A., Yates, P. A., Burrola, P., Ortuno, D., Vaidya, A., Jessell, T. M., Pfaff, S. L., O'Leary, D. D. and Lemke, G. (2000). Topographic mapping from the retina to the midbrain is controlled by relative but not absolute levels of EphA receptor signaling. *Cell* **102**, 77-88.
- Callaway, E. M. and Katz, L. C. (1992). Development of axonal arbors of layer 4 spiny neurons in cat striate cortex. *J. Neurosci.* **12**, 570-582.
- Chalupa, L. M. and Gunhan, E. (2004). Development of On and Off retinal pathways and retinogeniculate projections. *Prog. Retin. Eye Res.* **23**, 31-51.
- Cooper, M. S., Szeto, D. P., Sommers-Herivel, G., Topczewski, J., Solnica-Krezel, L., Kang, H. C., Johnson, I. and Kimelman, D. (2005). Visualizing morphogenesis in transgenic zebrafish embryos using BODIPY TR methyl ester dye as a vital counterstain for GFP. *Dev. Dyn.* **232**, 359-368.
- Copeland, N. G., Jenkins, N. A. and Court, D. L. (2001). Recombineering: a powerful new tool for mouse functional genomics. *Nat. Rev. Genet.* **2**, 769-779.
- Drenhaus, U., Morino, P. and Rager, G. (2004). Expression of axonin-1 in developing amacrine cells in the chick retina. *J. Comp. Neurol.* **468**, 496-508.
- Easter, S. S. and Nicola, G. N. (1996). The development of vision in the zebrafish, *Danio rerio*. *Dev. Biol.* **180**, 646-663.
- Evans, J. A. and Battelle, B. A. (1987). Histogenesis of dopamine-containing neurons in the rat retina. *Exp. Eye Res.* **44**, 407-414.
- Fadool, J. M., Fadool, D. A., Moore, J. C. and Linser, P. J. (1999). Characterization of monoclonal antibodies against zebrafish retina. *Invest. Ophthalmol. Vis. Sci.* **40**, 1251.
- Famiglietti, E. V., Jr and Kolb, H. (1976). Structural basis for ON- and OFF-center responses in retinal ganglion cells. *Science* **194**, 193-195.
- Famiglietti, E. V., Jr, Kaneko, A. and Tachibana, M. (1977). Neuronal architecture of on and off pathways to ganglion cells in carp retina. *Science* **198**, 1267-1269.
- Feldheim, D. A., Kim, Y. I., Bergemann, A. D., Frisen, J., Barbacid, M. and Flanagan, J. G. (2000). Genetic analysis of ephrin-A2 and ephrin-A5 shows their requirement in multiple aspects of retinocollicular mapping. *Neuron* **25**, 563-574.
- Galvez, J. M., Puelles, L. and Prada, C. (1977). Inverted (displaced) retinal amacrine cells and their embryonic development in the chick. *Exp. Neurol.* **56**, 151-157.
- Gunhan, E., Choudary, P. V., Landerholm, T. E. and Chalupa, L. M. (2002). Depletion of cholinergic amacrine cells by a novel immunotoxin does not perturb the formation of segregated on and off cone bipolar cell projections. *J. Neurosci.* **22**, 2265-2273.
- Gunhan-Agar, E., Kahn, D. and Chalupa, L. M. (2000). Segregation of on and off bipolar cell axonal arbors in the absence of retinal ganglion cells. *J. Neurosci.* **20**, 306-314.
- Hinds, J. W. and Hinds, P. L. (1978). Early development of amacrine cells in the mouse retina: an electron microscopic, serial section analysis. *J. Comp. Neurol.* **179**, 277-300.
- Hinds, J. W. and Hinds, P. L. (1983). Development of retinal amacrine cells in the mouse embryo: evidence for two modes of formation. *J. Comp. Neurol.* **213**, 1-23.
- Honjo, M., Tanihara, H., Suzuki, S., Tanaka, T., Honda, Y. and Takeichi, M. (2000). Differential expression of cadherin adhesion receptors in neural retina of the postnatal mouse. *Invest. Ophthalmol. Vis. Sci.* **41**, 546-551.
- Hu, M. and Easter, S. S. (1999). Retinal neurogenesis: the formation of the initial central patch of postmitotic cells. *Dev. Biol.* **207**, 309-321.
- Jontes, J. D., Buchanan, J. and Smith, S. J. (2000). Growth cone and dendrite dynamics in zebrafish embryos: early events in synaptogenesis imaged in vivo. *Nat. Neurosci.* **3**, 231-237.
- Kay, J. N., Roeser, T., Mumm, J. S., Godinho, L., Mrejeru, A., Wong, R. O. and Baier, H. (2004). Transient requirement for ganglion cells during assembly of retinal synaptic layers. *Development* **131**, 1331-1342.
- Koster, R. W. and Fraser, S. E. (2001). Tracing transgene expression in living zebrafish embryos. *Dev. Biol.* **233**, 329-346.
- Lee, M. Y., Shin, S. L., Han, S. H. and Chun, M. H. (1999). The birthdates of GABA-immunoreactive amacrine cells in the rat retina. *Exp. Brain Res.* **128**, 309-314.
- Lin, J. W., Biankin, A. V., Horb, M. E., Ghosh, B., Prasad, N. B., Yee, N. S., Pack, M. A. and Leach, S. D. (2004). Differential requirement for ptf1a in endocrine and exocrine lineages of developing zebrafish pancreas. *Dev. Biol.* **274**, 491-503.
- Link, B. A., Fadool, J. M., Malicki, J. and Dowling, J. E. (2000). The zebrafish young mutation acts non-cell-autonomously to uncouple differentiation from specification for all retinal cells. *Development* **127**, 2177-2188.
- Lohmann, C., Mumm, J. S., Morgan, J., Godinho, L., Schroeter, E. H., Stacy, R. C., Wong, W. T., Oakley, D. M. and Wong, R. O. (2005). Imaging the developing retina. In *Imaging in Neuroscience and Development* (ed. R. Yuste and A. Konnerth), pp. 171-183. New York: Cold Spring Harbor Laboratory Press.
- Luo, L. and O'Leary, D. D. M. (2005). Axon retraction and degeneration in development and disease. *Annu. Rev. Neurosci.* **28**, 127-156.
- Markram, H., Toledo-Rodriguez, M., Wang, Y., Gupta, A., Silberberg, G. and Wu, C. (2004). Interneurons of the neocortical inhibitory system. *Nat. Rev. Neurosci.* **5**, 793-807.
- Maslim, J. and Stone, J. (1988). Time course of stratification of the dendritic fields of ganglion cells in the retina of the cat. *Brain Res. Dev. Brain Res.* **44**, 87-93.
- McLaughlin, T., Hindges, R. and O'Leary, D. D. (2003). Regulation of axial patterning of the retina and its topographic mapping in the brain. *Curr. Opin. Neurobiol.* **13**, 57-69.
- Mumm, J. S., Godinho, L., Morgan, J. L., Oakley, D. M., Schroeter, E. H. and Wong, R. O. (2005). Laminar circuit formation in the vertebrate retina. *Prog. Brain Res.* **147**, 155-169.
- Nadarajah, B., Brunstrom, J. E., Grutzendler, J., Wong, R. O. and Pearlman, A. L. (2001). Two modes of radial migration in early development of the cerebral cortex. *Nat. Neurosci.* **4**, 143-150.
- Nadarajah, B., Alifragis, P., Wong, R. O. and Parnavelas, J. G. (2003). Neuronal migration in the developing cerebral cortex: observations based on real-time imaging. *Cereb. Cortex* **13**, 607-611.
- Nelson, R., Famiglietti, E. V., Jr and Kolb, H. (1978). Intracellular staining reveals different levels of stratification for on- and off-center ganglion cells in cat retina. *J. Neurophysiol.* **41**, 472-483.
- O'Leary, D. D. and Terashima, T. (1988). Cortical axons branch to multiple subcortical targets by interstitial axon budding: implications for target recognition and "waiting periods". *Neuron* **1**, 901-910.
- O'Leary, D. D. and McLaughlin, T. (2005). Mechanisms of retinotopic map development: Ephs, ephrins, and spontaneous correlated retinal activity. *Prog. Brain Res.* **147**, 43-65.
- Pang, J. J., Gao, F. and Wu, S. M. (2002). Segregation and integration of visual channels: layer-by-layer computation of ON-OFF signals by amacrine cell dendrites. *J. Neurosci.* **22**, 4693-4701.
- Peterson, R. E., Fadool, J. M., McClintock, J. and Linser, P. J. (2001). Muller cell differentiation in the zebrafish neural retina: evidence of distinct early and late stages in cell maturation. *J. Comp. Neurol.* **429**, 530-540.
- Prada, C., Puelles, L., Genis-Galvez, J. M. and Ramirez, G. (1987). Two modes of free migration of amacrine cell neuroblasts in the chick retina. *Anat. Embryol.* **175**, 281-287.
- Prada, C., Puga, J., Perez-Mendez, Lopez, L., and Ramirez, G. (1991). Spatial and temporal patterns of neurogenesis in the chick retina. *Eur. J. Neurosci.* **3**, 1187.
- Quesada, A., Prada, F., Armengol, J. A. and Genis-Galvez, J. M. (1981). Early morphological differentiation of the bipolar neurons in the chick retina. A Golgi analysis. *Anat. Histol. Embryol.* **10**, 328-341.
- Rapaport, D. H., Rakic, P. and LaVail, M. M. (1996). Spatiotemporal gradients of cell genesis in the primate retina. *Perspect. Dev. Neurobiol.* **3**, 147-159.
- Rapaport, D. H., Wong, L. L., Wood, E. D., Yasumura, D. and LaVail, M. M. (2004). Timing and topography of cell genesis in the rat retina. *J. Comp. Neurol.* **474**, 304-324.

- Reese, B. E. and Colello, R. J.** (1992). Neurogenesis in the retinal ganglion cell layer of the rat. *Neuroscience* **46**, 419-429.
- Reese, B. E., Raven, M. A., Giannotti, K. A. and Johnson, P. T.** (2001). Development of cholinergic amacrine cell stratification in the ferret retina and the effects of early excitotoxic ablation. *Vis. Neurosci.* **18**, 559-570.
- Ren, J. Q., McCarthy, W. R., Zhang, H., Adolph, A. R. and Li, L.** (2002). Behavioral visual responses of wild-type and hypopigmented zebrafish. *Vision Res.* **42**, 293-299.
- Schmitt, E. A. and Dowling, J. E.** (1999). Early retinal development in the zebrafish, *Danio rerio*: light and electron microscopic analyses. *J. Comp. Neurol.* **404**, 515-536.
- Shaner, N. C., Campbell, R. E., Steinbach, P. A., Giepmans, B. N., Palmer, A. E. and Tsien, R. Y.** (2004). Improved monomeric red, orange and yellow fluorescent proteins derived from *Discosoma* sp. red fluorescent protein. *Nat. Biotechnol.* **22**, 1567-1572.
- Somogyi, P. and Klausberger, T.** (2005). Defined types of cortical interneurone structure space and spike timing in the hippocampus. *J. Physiol.* **562**, 9-26.
- Stacy, R. C. and Wong, R. O.** (2003). Developmental relationship between cholinergic amacrine cell processes and ganglion cell dendrites of the mouse retina. *J. Comp. Neurol.* **456**, 154-166.
- Stell, W. K., Ishida, A. T. and Lightfoot, D. O.** (1977). Structural basis for on- and off-center responses in retinal bipolar cells. *Science* **198**, 1269-1271.
- Stuermer, C. A.** (1988). Retinotopic organization of the developing retinotectal projection in the zebrafish embryo. *J. Neurosci.* **8**, 4513-4530.
- Super, H., Martinez, A., Del Rio, J. A. and Soriano, E.** (1998). Involvement of distinct pioneer neurons in the formation of layer-specific connections in the hippocampus. *J. Neurosci.* **18**, 4616-4626.
- Wassle, H. and Boycott, B. B.** (1991). Functional architecture of the mammalian retina. *Physiol. Rev.* **71**, 447-480.
- Werblin, F., Roska, B. and Balya, D.** (2001). Parallel processing in the mammalian retina: lateral and vertical interactions across stacked representations. *Prog. Brain Res.* **131**, 229-238.
- Williams, R. R., Cusato, K., Raven, M. A. and Reese, B. E.** (2001). Organization of the inner retina following early elimination of the retinal ganglion cell population: effects on cell numbers and stratification patterns. *Vis. Neurosci.* **18**, 233-244.
- Wohrn, J. C., Puelles, L., Nakagawa, S., Takeichi, M. and Redies, C.** (1998). Cadherin expression in the retina and retinofugal pathways of the chicken embryo. *J. Comp. Neurol.* **396**, 20-38.
- Yamagata, M. and Sanes, J. R.** (1995). Lamina-specific cues guide outgrowth and arborization of retinal axons in the optic tectum. *Development* **121**, 189-200.
- Yamagata, M., Weiner, J. A. and Sanes, J. R.** (2002). Sidekicks: synaptic adhesion molecules that promote lamina-specific connectivity in the retina. *Cell* **110**, 649-660.
- Yazulla, S. and Studholme, K. M.** (2001). Neurochemical anatomy of the zebrafish retina as determined by immunocytochemistry. *J. Neurocytol.* **30**, 551-592.
- Zhang, D. R. and Yeh, H. H.** (1990). Histogenesis of corticotropin releasing factor-like immunoreactive amacrine cells in the rat retina. *Brain Res. Dev. Brain Res.* **53**, 194-199.